



# Mapping CH<sub>4</sub> : CO<sub>2</sub> ratios in Los Angeles with CLARS-FTS from Mount Wilson, California

K. W. Wong<sup>1</sup>, D. Fu<sup>1</sup>, T. J. Pongetti<sup>1</sup>, S. Newman<sup>2</sup>, E. A. Kort<sup>4</sup>, R. Duren<sup>1</sup>, Y.-K. Hsu<sup>3</sup>, C. E. Miller<sup>1</sup>, Y. L. Yung<sup>2</sup>, and S. P. Sander<sup>1</sup>

<sup>1</sup>Jet Propulsion Laboratory, California Institute of Technology, Pasadena, California, USA

<sup>2</sup>Division of Geological and Planetary Sciences, California Institute of Technology, Pasadena, California, USA

<sup>3</sup>California Air Resources Board, Sacramento, California, USA

<sup>4</sup>Department of Atmospheric, Oceanic and Space Sciences, University of Michigan, Ann Arbor, Michigan, USA

Correspondence to: K. W. Wong (clare.wong@jpl.nasa.gov)

Received: 23 May 2014 – Published in Atmos. Chem. Phys. Discuss.: 26 June 2014

Revised: 16 September 2014 – Accepted: 18 October 2014 – Published: 12 January 2015

**Abstract.** The Los Angeles megacity, which is home to more than 40 % of the population in California, is the second largest megacity in the United States and an intense source of anthropogenic greenhouse gases (GHGs). Quantifying GHG emissions from the megacity and monitoring their spatiotemporal trends are essential to be able to understand the effectiveness of emission control policies. Here we measure carbon dioxide (CO<sub>2</sub>) and methane (CH<sub>4</sub>) across the Los Angeles megacity using a novel approach – ground-based remote sensing from a mountaintop site. A Fourier transform spectrometer (FTS) with agile pointing optics, located on Mount Wilson at 1.67 km above sea level, measures reflected near-infrared sunlight from 29 different surface targets on Mount Wilson and in the Los Angeles megacity to retrieve the slant column abundances of CO<sub>2</sub>, CH<sub>4</sub> and other trace gases above and below Mount Wilson. This technique provides persistent space- and time-resolved observations of path-averaged dry-air GHG concentrations, XGHG, in the Los Angeles megacity and simulates observations from a geostationary satellite. In this study, we combined high-sensitivity measurements from the FTS and the panorama from Mount Wilson to characterize anthropogenic CH<sub>4</sub> emissions in the megacity using tracer–tracer correlations. During the period between September 2011 and October 2013, the observed XCH<sub>4</sub> : XCO<sub>2</sub> excess ratio, assigned to anthropogenic activities, varied from 5.4 to 7.3 ppb CH<sub>4</sub> (ppm CO<sub>2</sub>)<sup>-1</sup>, with an average of 6.4 ± 0.5 ppb CH<sub>4</sub> (ppm CO<sub>2</sub>)<sup>-1</sup> compared to the value of 4.6 ± 0.9 ppb CH<sub>4</sub> (ppm CO<sub>2</sub>)<sup>-1</sup> expected from the California Air Resources Board (CARB) bottom-up emis-

sion inventory. Persistent elevated XCH<sub>4</sub> : XCO<sub>2</sub> excess ratios were observed in Pasadena and in the eastern Los Angeles megacity. Using the FTS observations on Mount Wilson and the bottom-up CO<sub>2</sub> emission inventory, we derived a top-down CH<sub>4</sub> emission of 0.39 ± 0.06 Tg CH<sub>4</sub> year<sup>-1</sup> in the Los Angeles megacity. This is 18–61 % larger than the state government's bottom-up CH<sub>4</sub> emission inventory and consistent with previous studies.

## 1 Introduction

The Los Angeles megacity – a sprawling urban expanse of ~ 100 km × 100 km and 15 million people – covers only ~ 4 % of California's land area but is home to more than 43 % of its population and dominates the state's anthropogenic greenhouse gas (GHG) emissions. By treating the megacity as an effective “point source”, we can quantify trends in this critical component of the state's GHG emissions and support California's goal of reducing GHG emissions to the 1990 level by 2020 mandated by the state's Global Warming Solutions Act of 2006 (AB32).

Emissions of carbon dioxide (CO<sub>2</sub>) and methane (CH<sub>4</sub>) in the Los Angeles megacity originate largely from different economic sectors and are expected to have distinctly different spatial and temporal patterns. Anthropogenic CO<sub>2</sub> is derived mainly from motor vehicle exhaust (transportation), exhibiting strong diurnal variability and weak seasonal variability, and from natural-gas-fueled power plants (power) with a

few large stationary emitters and significant seasonal variability. Overall CO<sub>2</sub> emissions for transportation and power plants are known to within  $\pm 10\%$  from fuel usage and emission factors (de la Rue du Can et al., 2008). On the other hand, the CH<sub>4</sub> emissions budget is highly uncertain and contains significant but poorly quantified emissions from a variety of sources such as landfills and wastewater treatment plants (waste), oil and gas production, storage and delivery infrastructure (power and residential), dairy farms (agriculture) and geologic seeps (geology). Recent studies estimating CH<sub>4</sub> emissions from atmospheric observations have shown that the bottom-up total CH<sub>4</sub> emissions inventory in the Los Angeles megacity have uncertainties of 30% to > 100% (Wunch et al., 2009; Hsu et al., 2010; Wennberg et al., 2012; Jeong et al., 2013; Peischl et al., 2013). Atmospheric observations may be used to characterize spatial and temporal patterns in CO<sub>2</sub> and CH<sub>4</sub> within the Los Angeles megacity and to provide initial estimates of sectoral emissions attribution.

Wunch et al. (2009) demonstrated the estimation of GHGs using the ground-based column measurements acquired at a Total Carbon Column Observing Network (TCCON) station in Pasadena, California, in the Los Angeles basin. Since column measurements are relatively insensitive to boundary layer height variations and are less influenced by local surface sources than ground in situ measurements, they should be more representative of the area. They reported that the bottom-up CH<sub>4</sub> emissions for the Los Angeles megacity are less than half of the top-down CH<sub>4</sub> emissions. The large uncertainty in the bottom-up CH<sub>4</sub> emission inventory in the Los Angeles megacity has also been supported by the CH<sub>4</sub> : CO<sub>2</sub> ratios observed by aircraft campaigns, ARCTAS-CARB (Arctic Research of the Composition of the Troposphere from Aircraft and Satellites—California Air Resources Board) in 2008 and CalNex (California Nexus) in 2010 (Wennberg et al., 2012; Peischl et al., 2013), and in situ observations on Mount Wilson (Hsu et al., 2010).

Despite the potential of atmospheric observations to quantify the emissions of CH<sub>4</sub>, CO<sub>2</sub> and other GHGs in the Los Angeles megacity, they have certain limitations for tracking long-term GHG emissions. Kort et al. (2013) showed that surface in situ observations from no single site within or adjacent to the Los Angeles megacity accurately capture the emissions from the entire region. Similarly, ground-based total column measurements from Pasadena also lack sensitivity to emissions from across the entire region. Kort et al. (2013) concluded that the size and complexity of the Los Angeles megacity urban dome require a network of at least eight strategically located continuous surface in situ observing sites to quantify and track GHG emissions over time with  $\sim 10\%$  uncertainty. However, this minimum network would have limited capabilities to identify and isolate emissions from specific sectors and/or localized sources. It is therefore necessary to develop a robust, long-term measurement solution that resolves emissions in the Los Angeles megacity both spatially and temporally.

The present study reports GHG measurements of the Los Angeles megacity from an elevated vantage point, the California Laboratory for Atmospheric Remote Sensing (CLARS), located on Mt. Wilson at an altitude of 1670 m a.s.l. and overlooking the Los Angeles megacity (Fig. 1). We present column-averaged dry-air mole fraction CO<sub>2</sub> (XCO<sub>2</sub>) and CH<sub>4</sub> (XCH<sub>4</sub>) measurements for 29 reflection points distributed across Los Angeles. The measurements cover daytime hours for the 2-year period between 2011 and 2013. We determine the enhancements in XCH<sub>4</sub> and XCO<sub>2</sub> in the basin compared to background levels, and we use the spatial distribution of the XCH<sub>4</sub>(excess) : XCO<sub>2</sub>(excess) ratio to quantify emissions in the megacity. We compare our results to column, surface in situ and aircraft in situ observations and compare our derived megacity CH<sub>4</sub> emissions estimates with the results from previous studies.

CLARS provides a unique long-term record that simulates geostationary satellite observations (GEO) for the Los Angeles basin. CLARS maps the diurnal variability of both XCO<sub>2</sub> and XCH<sub>4</sub> within the Los Angeles urban dome with hourly timescales. It has functioned operationally since 2011, and its sustained measurements are yielding insights into the scientific value of GEO GHG monitoring, as well as helping to define GEO-based GHG measurement requirements. Existing and future satellite instruments such as the Tropospheric Emission Spectrometer (TES) onboard Aura, TANSO-FTS onboard the Greenhouse Gases Observing Satellite (GOSAT) and the Orbiting Carbon Observatory-2 (OCO-2) all sample from sun-synchronous low Earth orbits. These platforms sample globally but return to the same measurement point on the Earth infrequently, with repeat cycles ranging from days to weeks. In contrast, GEO measurements, such as those from the proposed Geostationary Fourier Transform Spectrometer (GEO-FTS), map the complete field of regard with high spatial resolution (< 10 km horizontal resolution) many times per day (Key et al., 2012). Measurements from a mountaintop location, such as CLARS, provide similar spatial and temporal resolution to GEO measurements but with a larger viewing zenith angle which enhances the optical path in the planetary boundary layer (PBL). We also demonstrate that simultaneous XCH<sub>4</sub> and XCO<sub>2</sub> measurements are essential to quantify megacity GHG emissions and also provide critical information from which to attribute emissions from different economic sectors.

## 2 Measurement technique

### 2.1 CLARS-FTS

A Jet Propulsion Laboratory (JPL)-built Fourier transform spectrometer (FTS) has been deployed since 2010 at the CLARS facility on Mount Wilson at an altitude of 1670 m a.s.l. overlooking the Los Angeles megacity (Fig. 1).

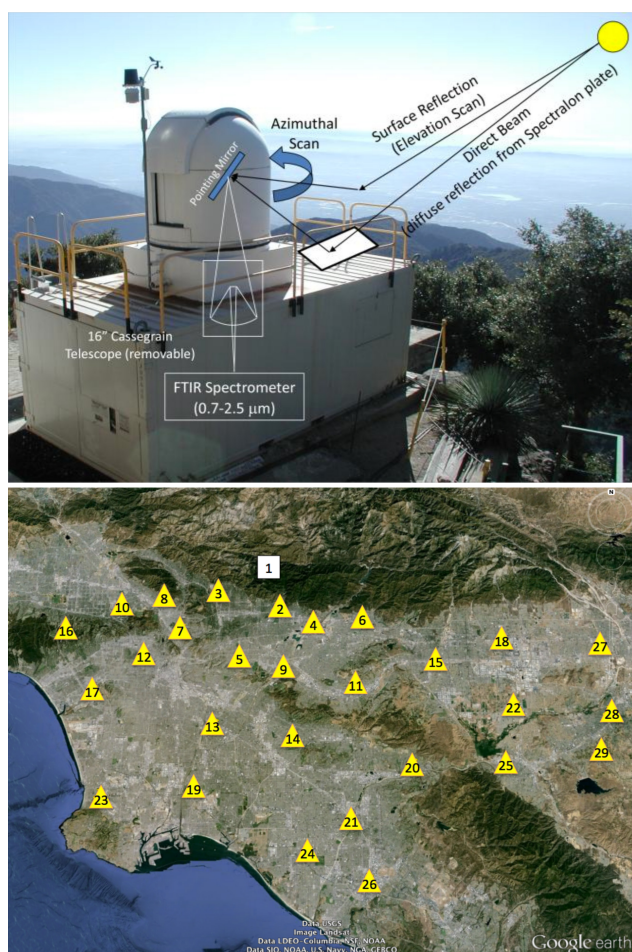


**Figure 1.** The CLARS-FTS on Mount Wilson (top) and its 29 reflection points on Mount Wilson and in the Los Angeles megacity (bottom). Reflection points are labeled in the order of increasing distance from the FTS. Information of the reflection points is given in Table 1. A small fraction of the central Los Angeles megacity area cannot be viewed from Mount Wilson due to a nearby mountain peak.

The FTS operates in two modes: the Spectralon Viewing Observations (SVO) and the Los Angeles Basin Surveys (LABS). In the SVO mode, the FTS points at a Spectralon<sup>®</sup> plate placed immediately below the FTS telescope to quantify the total column CO<sub>2</sub> and CH<sub>4</sub> above the Los Angeles megacity (above 1670 m and the basin PBL height). The SVO measurements represent approximately free tropospheric background levels. In the LABS mode, the FTS points downward at 28 geographical points in the basin acquiring spectra from reflected sunlight in the near-infrared region (Table 1). Our measurement technique from Mount Wilson mimics satellite observations that measure surface reflectance from space or atmospheric absorptions of GHGs along the optical path – (1) from the sun to the surface and (2) from the surface to the instrument. The locations of the reflection points are selected to provide the best coverage of

the megacity (Fig. 1). In addition, reflection points are chosen with uniform surface albedo across the spectrometer field of view using a near-infrared camera. Reflection points sample from the San Bernardino Mountains in the east to the Pacific coast in the west, and from the base of the San Gabriel Mountains in the north to Long Beach Harbor and Orange County in the south. For a typical PBL height, the geometric slant paths within the PBL range from  $\sim 4$  km (Santa Anita Park) to  $\sim 39$  km (Lake Mathews). The points in Table 1 are the baseline raster pattern, but they can be modified easily if desired. In the standard measurement cycle, the FTS points at these 28 reflection points and performs four SVO measurements per cycle. There are five to eight measurement cycles per day depending on the time of the year.

The spectral resolution used in the CLARS-FTS measurement is  $0.12\text{ cm}^{-1}$ , with an angular radius of the field of view of  $0.5\text{ mrad}$ . The footprints in the Los Angeles megacity are ellipses with surface area ranging from  $0.04$  to  $21.62\text{ km}^2$  (Table 1). The pointing calibration procedure is designed to maximize pointing accuracy (Fu et al., 2014). Pointing uncertainties are primarily due to errors arising from gimbals tilt and minor position-dependent flexing of the pointing system structure. After pointing calibration corrections are applied, the CLARS-FTS pointing system has a total uncertainty of  $0.17^\circ$  ( $1\sigma$ ) in azimuth, which is about 30 % of the CLARS-FTS field of view. This results in a ground distance error of about 60 m for a reflection point located 20 km from Mount Wilson. Uncertainty is  $0.045^\circ$  ( $1\sigma$ ) in elevation – that is, 8 % of the CLARS-FTS field of view – resulting in a ground distance error of about 16 m for a target that is 20 km from Mount Wilson. Details concerning the CLARS-FTS design, operation and calibration are described in Fu et al. (2014).

## 2.2 Data processing

The CLARS interferogram processing program (CLARS-IPP) converts the recorded interferograms into spectra. The CLARS-IPP also corrects for solar intensity variations. Twelve single-scan spectra are co-added over a period of 3 min for each reflection point to achieve a spectral signal-to-noise ratio (SNR) of  $\sim 300:1$  for LABS measurements and  $\sim 450:1$  for SVO measurements. The instrument line shape (ILS) of the CLARS-FTS is characterized using an external lamp and an HCl gas cell. Our experiment works on a simple Beer–Lambert principle where the number densities of CO<sub>2</sub> and CH<sub>4</sub> are proportional to the optical depths measured for rotationally resolved near-infrared absorption spectra. Slant column density (SCD), the total number of absorbing molecule per unit area along the Sun–Earth–instrument optical path, is retrieved for CO<sub>2</sub> and CH<sub>4</sub> using a modified version of the Gas Fitting tool (GFIT) algorithm (Wunch et al., 2011; Fu et al., 2014). Descriptions of the CLARS-FTS data processing and retrieval algorithm are included in Fu et al. (2014). In the present analysis, we retrieve CO<sub>2</sub> from bands at  $1.6\text{ }\mu\text{m}$ , CH<sub>4</sub> at  $1.67\text{ }\mu\text{m}$  and O<sub>2</sub> at  $1.27\text{ }\mu\text{m}$ . The re-

**Table 1.** List of the 29 reflection points on Mount Wilson and in the Los Angeles megacity.

	Target	Latitude	Longitude	Slant distance from FTS (km)	Slant path* in PBL (km)	Footprint (km <sup>2</sup> )
1	Spectralon <sup>®</sup> , Mount Wilson	34.22	−118.06	0.01	0	0
2	Santa Anita Park	34.14	−118.04	9.2	4.2	0.04
3	West Pasadena	34.17	−118.17	11.5	5.9	0.09
4	Santa Fe Dam	34.11	−117.97	14.9	6.8	0.17
5	East Los Angeles	34.05	−118.12	20.2	9.2	0.41
6	Fwy 210	34.12	−117.87	20.9	10.1	0.49
7	Downtown (near)	34.10	−118.23	21.1	9.6	0.47
8	Glendale	34.15	−118.27	21.4	10.0	0.50
9	Fwys 60 and 605	34.03	−118.03	21.7	9.5	0.49
10	Universal City	34.14	−118.35	28.8	13.4	1.23
11	Fwy 60, City of Industry	34.00	−117.88	29.6	13.7	1.33
12	Downtown (far)	34.05	−118.31	29.7	12.9	1.25
13	Downey	33.93	−118.16	33.9	14.5	1.84
14	La Mirada	33.91	−118.01	35.2	15.3	2.09
15	Pomona	34.04	−117.73	36.7	18.1	2.70
16	Santa Monica Mountains	34.09	−118.47	40.9	20.2	3.74
17	Marina Del Rey	33.99	−118.40	41.0	17.3	3.22
18	Rancho Cucamonga	34.08	−117.59	46.1	24.0	5.66
19	Long Beach	33.82	−118.20	46.5	19.6	4.70
20	North Orange County	33.86	−117.78	47.8	21.3	5.38
21	Angels Stadium	33.80	−117.88	49.8	21.5	5.89
22	Norco	33.96	−117.57	53.5	25.3	8.01
23	Palos Verdes	33.81	−118.37	54.2	23.7	7.70
24	Huntington Beach	33.72	−117.98	56.2	23.8	8.32
25	Corona	33.87	−117.60	56.0	28.8	10.71
26	Orange Country Airport	33.68	−117.86	63.3	26.7	11.86
27	Fontana	34.07	−117.39	64.3	33.8	15.46
28	Riverside	33.95	−117.39	68.5	34.1	17.75
29	Lake Mathews	33.88	−117.42	70.7	39.1	21.62

\* Slant paths in PBL are estimated assuming a uniform PBL height of 700 m, which was the average PBL height observed during CalNex 2010.

trieved SCDs are converted to slant-column-averaged dry-air mole fractions, XCO<sub>2</sub> and XCH<sub>4</sub>, by normalizing to SCD<sub>O<sub>2</sub></sub> (Eq. 1).

$$X_{\text{GHG}} = \frac{\text{SCD}_{\text{GHG}}}{\text{SCD}_{\text{O}_2}} \times 0.2095 \quad (1)$$

This method has been shown to improve the precision of XCO<sub>2</sub> and XCH<sub>4</sub> retrievals since SCD<sub>O<sub>2</sub></sub> retrieval effectively cancels out first-order path length, instrumental and retrieval algorithm errors (Washenfelder and Wennberg, 2003; Washenfelder et al., 2006; Wunch et al., 2011; Fu et al., 2014). Measurement precisions are 0.3 ppm for XCO<sub>2</sub> (~0.1 %) and 2.5 ppb for XCH<sub>4</sub> (~0.1 %) for the SVO measurements and 0.6 ppm for XCO<sub>2</sub> (~0.1 %) and 4.7 ppb for XCH<sub>4</sub> (~0.2 %) for the LABS measurements. Estimated measurement accuracies are <3.1 % for XCO<sub>2</sub> and <6.0 % for XCH<sub>4</sub>, driven mainly by uncertainties in laboratory spectral line parameters.

### 2.3 Data filtering

Poor air quality in Los Angeles causes visibility reduction due to aerosol scattering. While the impact of aerosol scattering is significantly lower in the infrared than the visible and ultraviolet spectral regions, CLARS-FTS trace gas retrievals can be affected by aerosols due to the long optical path length in the boundary layer. In addition to aerosol, the Los Angeles megacity is often affected by morning marine layer fog and low clouds, which influence the data quality.

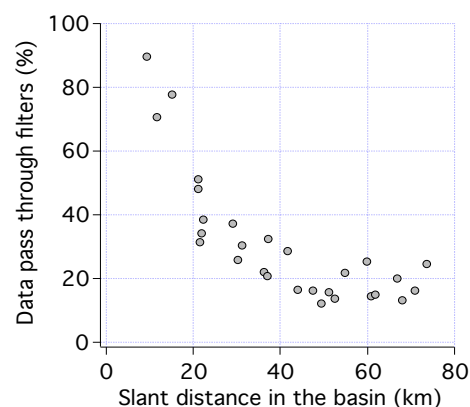
Individual retrievals are analyzed with multiple post-processing filters to ensure data quality, similar to the QA/QC (quality assurance/quality control) filters adopted in the Atmospheric CO<sub>2</sub> Observations from Space (ACOS)-GOSAT data processing (O'Dell et al., 2012; Crisp et al., 2012; Mandrake et al., 2013). Table 2 summarizes the filtering criteria. Data with poor spectral fitting quality – such as with large solar zenith angle (SZA), low SNR and/or large fitting residual root mean square (rms) errors – are removed. Data are also screened for clouds and aerosols using the ratio of retrieved

**Table 2.** Data filter criteria.

Filter	Criteria
High clouds	SVO O <sub>2</sub> SCD <sub>retrieved</sub> : O <sub>2</sub> SCD <sub>geometric</sub> > 1.1 or < 1
Low clouds and/or aerosol	LABS O <sub>2</sub> SCD <sub>retrieved</sub> : O <sub>2</sub> SCD <sub>geometric</sub> > 1.1 or < 0.9
Large SZA	SZA > 70°
Low SNR	SNR < 100
Poor spectral fitting	Fitting residual rms > 1 standard deviation above average

to geometric oxygen SCDs as the criterion. The geometric oxygen SCD is calculated using surface pressure from National Center for Environmental Prediction (NCEP) reanalysis data assuming hydrostatic equilibrium, a constant oxygen dry-air volume mixing ratio of 0.2095 along the optical path and no scattering or absorption occurs (Fu et al., 2014). Because oxygen is well mixed in the atmosphere, deviations in the retrieved oxygen SCD from the geometric oxygen SCD indicate variations of the light path due to clouds and/or aerosols, assuming deviations are larger than the retrieval uncertainty, that is, < 0.3 % for SVO measurements and ~ 0.5 % for LABS measurements (errors represent precisions only). For high clouds, data are filtered out when the corresponding SVO oxygen SCD ratio is less than 1 or greater than 1.1. For low clouds, data with retrieved target oxygen SCD deviating more than 10 % from the geometric value are removed. We use the same criteria to take out data with heavy aerosol loading, which leads to significant modification in the light path. This filtering approach is equivalent to that used by ACOS, which compares the retrieved surface pressure to reanalysis data (O'Dell et al., 2012). As a result of our data filters, more data are removed for reflection points located further away from Mount Wilson since these measurements have larger fractions of their optical paths in the PBL and are more likely to encounter substantial scattering (Fig. 2).

Numerous studies have shown that aerosol scattering in the atmosphere has an impact on the retrieved trace gas mixing ratios from space-based observations in the near infrared (Aben et al., 2007; Yoshida et al., 2011; Crisp et al., 2012). Zhang et al. (2015) used a numerical two-stream radiative transfer model (RTM) validated against the Linearized Pseudo-spherical Vector Discrete Ordinate Radiative Transfer (VLIDORT) full-physics RTM (Spurr et al., 2006) to estimate the expected biases in the retrieved values of XCO<sub>2</sub> and XCH<sub>4</sub> from CLARS observations. The model was used to set the value for the CLARS aerosol filter criterion in terms of the ratio of measured to geometric optical path length derived from the 1.27 μm absorption band of molecular oxygen (see Sect. 4.1).

**Figure 2.** Percent of data points that pass through our data filters as a function of slant distance in the Los Angeles megacity.

### 3 Observations

#### 3.1 Diurnal variations of XCO<sub>2</sub> and XCH<sub>4</sub> : SVO vs. LABS

Due to the difference in the measurement geometry between the SVO mode and the LABS mode, the diurnal patterns of XCO<sub>2</sub> and XCH<sub>4</sub> differ significantly. Figure 3 shows an example of the diurnal variations of raw and filtered XCO<sub>2</sub> and XCH<sub>4</sub> measurements for the SVO mode, and the LABS west Pasadena and Santa Anita Park targets from ~ 8:30 to ~ 16:30 LT on 7 consecutive days during the period of 5–11 May 2012. The SVO retrievals showed constant path-averaged mixing ratios of about 390 ppm XCO<sub>2</sub> and 1700 ppb XCH<sub>4</sub> during this period. The constant diurnal pattern was observed because the FTS is located most of the time above the planetary boundary layer where sources are located (Newman et al., 2013). Therefore the SVO measurements do not capture variations of atmospheric CO<sub>2</sub> and CH<sub>4</sub> mixing ratio due to emissions in the Los Angeles megacity.

On the other hand, the west Pasadena and Santa Anita Park reflection points exhibited strong diurnal signals in XCO<sub>2</sub> and XCH<sub>4</sub>, with a minimum typically in the early morning of around 405–410 ppm for XCO<sub>2</sub> and 1800–1900 ppb for XCH<sub>4</sub> and a maximum of up to 420 ppm for XCO<sub>2</sub> and 1950 ppb for XCH<sub>4</sub> at noon or in the early afternoon. Variability in CO<sub>2</sub> and CH<sub>4</sub> emissions and atmospheric transport resulted in daily ranges of variation of 10–30 ppm XCO<sub>2</sub> and

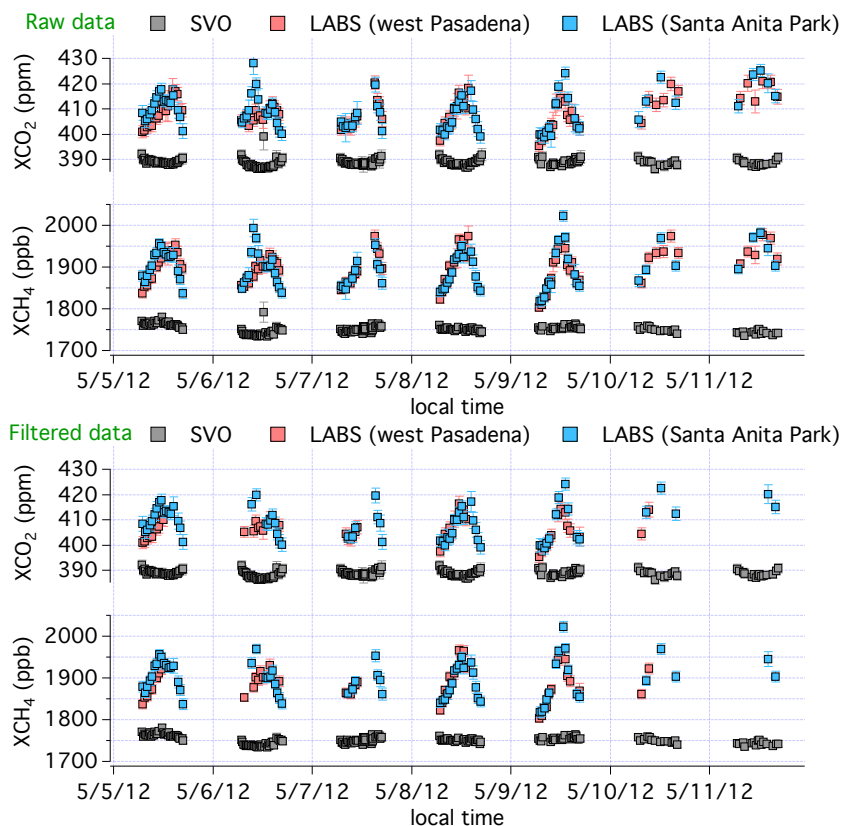


**Figure 3.** Upper panel shows the raw data, and bottom panel shows the filtered data. Diurnal variations of SVO (grey) and LABS, west Pasadena (red) and Santa Anita Park (blue), and XCO<sub>2</sub> and XCH<sub>4</sub> from around 8:30 to 16:30 on 7 consecutive days in May 2012. Error bars represent the rms of the retrieval spectral fitting residual. Bad data points, such as data taken in the cloudy morning of 11 May, were removed from the filtered data set. From 5 to 9 May the FTS was operated in the target mode, taking alternate measurements between SVO, west Pasadena and Santa Anita Park. On 10 and 11 May the standard measurement cycle was performed, resulting in fewer measurements from each target.

100–200 ppb XCH<sub>4</sub> during the period of 5–11 May 2012. With a typical boundary layer height, the west Pasadena and the Santa Anita Park measurements sample horizontally over a few kilometers in the PBL and are therefore sensitive to emission signatures. The buildup of XCO<sub>2</sub> and XCH<sub>4</sub> in the morning and the falloff in the afternoon are due to a combination of accumulation of emissions and dilution/advection processes in the basin. Similar diurnal patterns of XCO<sub>2</sub> and XCH<sub>4</sub> (that is, peak at noon or early afternoon) have been observed in Pasadena by a TCCON station (Wunch et al., 2009). However, the column enhancements observed by TCCON are typically less than 2–3 ppm in XCO<sub>2</sub> and 20–40 ppb in XCH<sub>4</sub>. These enhancements are significantly smaller than those derived from the CLARS-FTS measurements which have a longer optical path within the PBL compared with TCCON at the same SZA.

Variations in PBL height do not affect the diurnal profile of XCO<sub>2</sub> and XCH<sub>4</sub> as they would in in situ measurements, in which diurnal variation is often characterized by GHG concentration peaks in the morning and evening when the PBL is

shallow and a minimum in midday when the PBL has grown (Newman et al., 2013). This is because XCO<sub>2</sub> and XCH<sub>4</sub> are derived from the slant column abundance along the CLARS-FTS optical paths. This is valid as long as the PBL height is below Mount Wilson. Since the PBL typically locates below Mount Wilson (Newman et al., 2013), this is a major advantage of column measurements over in situ measurements.

### 3.2 Slopes of derived CH<sub>4</sub>–CO<sub>2</sub> correlations

Several studies have reported strong correlations between CH<sub>4</sub> and CO<sub>2</sub> measured in the PBL in source regions (Peischl et al., 2013; Wennberg et al., 2012; Wunch et al., 2009; S. Newman, personal communication, 2014). Slopes of CH<sub>4</sub>–CO<sub>2</sub> correlation plots have been identified with local emission ratios for the two gases. Since the uncertainty in CH<sub>4</sub> emissions is considerably larger than that in CO<sub>2</sub> emissions, we may use the correlation slope to reduce the CH<sub>4</sub> emission uncertainties. A few assumptions are used when quantifying CH<sub>4</sub> emission based on the CH<sub>4</sub>–CO<sub>2</sub> correlation. These assumptions will be discussed in Sect. 4.1 of the paper. In

this study, we determined the spatial variation of CH<sub>4</sub> : CO<sub>2</sub> ratios originating from CLARS-FTS measurements between September 2011 and October 2013. It is first necessary to remove the background variations in CO<sub>2</sub> and CH<sub>4</sub> in order to calculate the concentration anomalies resulting from emissions in the PBL. Different approaches to deriving the background concentrations were considered, including using the early morning, daily minimum and daily average XGHG for each reflection point. However, because of variations in the yield of LABS data passing through the data filters, biases may be introduced into the background estimation by these methods. As a result, we determined that the SVO observations, which have a very small diurnal variation, are the most appropriate background reference values for the CLARS LABS measurements. The excess XCO<sub>2</sub> and XCH<sub>4</sub> above background in the Los Angeles megacity are simply calculated by subtracting the SVO observations from the LABS observations (Eq. 2).

$$\text{XGHG}_{(\text{XS})} = \text{XGHG}_{\text{LABS}} - \text{XGHG}_{\text{SVO}} \quad (2)$$

We used orthogonal distance regression (ODR) analysis, which considers uncertainties in both XCH<sub>4(XS)</sub> and XCO<sub>2(XS)</sub>, to quantify the emissions of CH<sub>4</sub>-relative CO<sub>2</sub> in the Los Angeles megacity. Using this approach, we find values of  $7.3 \pm 0.1$  ppb CH<sub>4</sub> (ppm CO<sub>2</sub>)<sup>-1</sup> for the west Pasadena reflection point and  $6.1 \pm 0.1$  ppb CH<sub>4</sub> (ppm CO<sub>2</sub>)<sup>-1</sup> for the Santa Anita Park reflection point. Figure 4 illustrates the tight correlations found between XCH<sub>4(XS)</sub> and XCO<sub>2(XS)</sub> for each reflection point. The tight correlations imply that there is not a substantial difference in the emission ratio of the two GHGs during the measurement period from 2011 to 2013. XCH<sub>4(XS)</sub> and XCO<sub>2(XS)</sub> should be poorly correlated with each other if their emission ratio varies largely over time, assuming the correlation is mainly driven by emissions.

Table 3 lists the correlation slopes and their uncertainties for the 28 basin reflection points. Figure 5 maps the observed XCH<sub>4(XS)</sub> / XCO<sub>2(XS)</sub> correlation slopes (in units of ppb CH<sub>4</sub> (ppm CO<sub>2</sub>)<sup>-1</sup>) across the Los Angeles megacity using natural neighbor interpolation (Sibson, 1981). The mean  $\pm 1$  standard deviation for all 28 reflection points was  $6.4 \pm 0.5$  ppb CH<sub>4</sub> (ppm CO<sub>2</sub>)<sup>-1</sup>, with individual values ranging from 5.4 to 7.3 ppb CH<sub>4</sub> (ppm CO<sub>2</sub>)<sup>-1</sup>. Elevated XCH<sub>4(XS)</sub> / XCO<sub>2(XS)</sub> ratios were observed in west Pasadena and in the eastern side of the Los Angeles megacity.

Spatial gradients among reflection points became weaker as distance from Mount Wilson increased. Stronger spatial gradients were observed among the closer reflection points in the basin – that is, west Pasadena, Santa Anita Park and east Los Angeles – while weaker spatial gradients were observed among the more distant reflection points, such as Long Beach, Marina Del Rey and north Orange County. Measurements were averaged over a much longer slant path for the more distant reflection points, compared to the nearby

**Table 3.** List of correlation slopes of XCH<sub>4(XS)</sub> : XCO<sub>2(XS)</sub> and their uncertainties (1 standard deviation) observed by the CLARS-FTS during the period of September 2011 and October 2013.

Target	XCH <sub>4(xs)</sub> / XCO <sub>2(xs)</sub> (ppb/ppm)	Uncertainties* (ppb/ppm)
Santa Anita Park	6.09	0.05
West Pasadena	7.28	0.09
Santa Fe Dam	5.85	0.12
East Los Angeles	5.99	0.15
Fwy 210	6.26	0.20
Downtown (near)	6.42	0.21
Glendale	6.04	0.20
Fwys 60 and 605	7.34	0.31
Universal City	6.47	0.28
Fwy 60, City of Industry	7.25	0.41
Downtown (far)	6.33	0.23
Downey	6.24	0.29
La Mirada	7.13	0.35
Pomona	6.52	0.25
Santa Monica Mountains	6.55	0.33
Marina Del Rey	6.75	0.27
Rancho Cucamonga	5.35	0.15
Long Beach	6.18	0.28
North Orange County	6.41	0.35
Angels Stadium	6.65	0.39
Norco	6.87	0.31
Palos Verdes	6.59	0.34
Huntington Beach	6.10	0.24
Corona	6.40	0.30
Orange Country Airport	5.99	0.29
Fontana	6.18	0.23
Riverside	6.40	0.32
Lake Mathews	5.99	0.23

\* The uncertainties include only fitting uncertainties. Systematic uncertainties of  $\sim 4\%$  were not taken into account here (Fu et al., 2014).

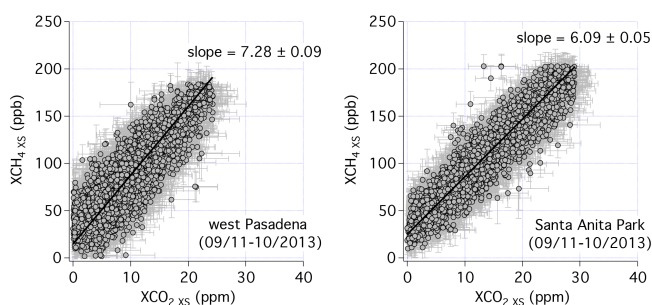


**Figure 4.** Correlations between XCH<sub>4(XS)</sub> (ppb) and XCO<sub>2(XS)</sub> (ppm) for west Pasadena and Santa Anita Park during the period of September 2011 and October 2013.

reflection points, making the measurements for the more distant reflection points less sensitive to local/point sources. Bootstrap analysis (Efron and Tibshirani, 1993) was performed to make sure that the spatial variations of the correlation slopes were not a result of sampling bias among the 28 reflection points. The uncertainties in the correlation slopes became larger with increasing distance from Mount Wilson

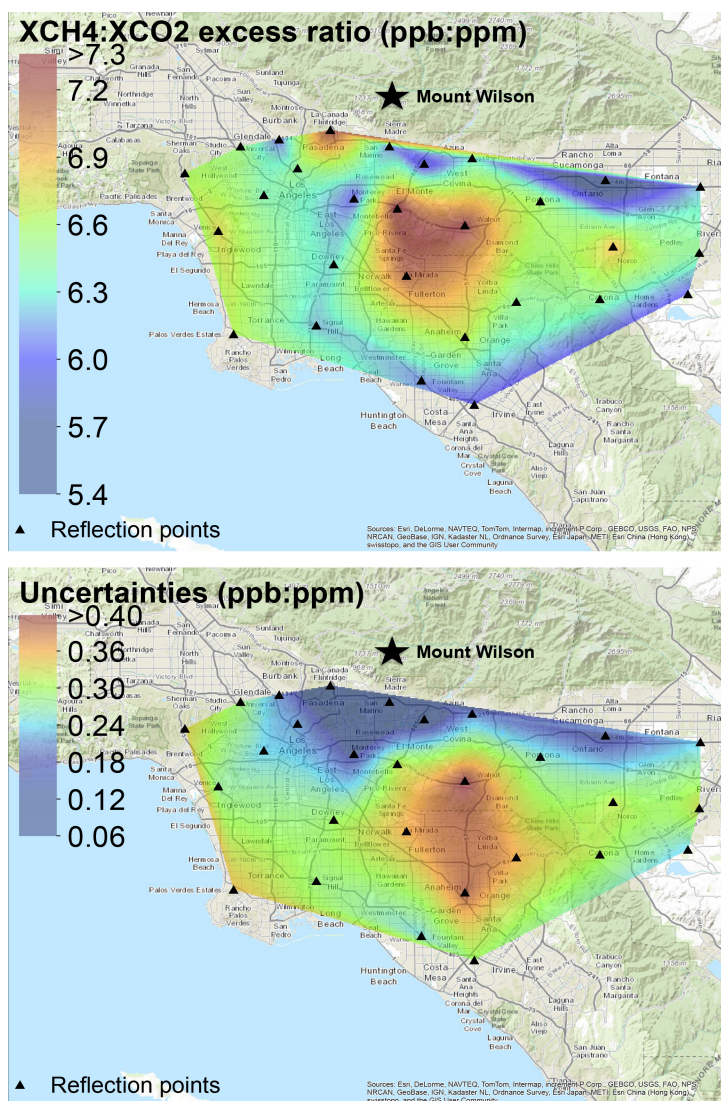


**Figure 5.** Maps of correlation slopes of the  $X\text{CH}_4(X_S) : X\text{CO}_2(X_S)$  ratio (top) and their uncertainties (1 standard deviation) (bottom) in the Los Angeles megacity observed by the CLARS-FTS during the period of September 2011 and October 2013.

due to the decreased data quality, as the measurement path in the Los Angeles megacity became longer. (More data were filtered out for targets further from the instrument, mostly because of aerosol loading.)

The CLARS-FTS observations in west Pasadena are in good agreement with TCCON measurements at the Jet Propulsion Laboratory, which showed a ratio of  $7.8 \pm 0.8$  ppb ppb CH<sub>4</sub> (ppm CO<sub>2</sub>)<sup>-1</sup> (Wunch et al., 2009). Subtle differences between the TCCON and the CLARS-FTS are due to the relative change in the ratio over time, difference measurement geometry and/or the different approach in determining the excess ratio. A number of in situ ground and aircraft measurements of CO<sub>2</sub> and CH<sub>4</sub> have been performed recently with the goal of quantifying GHG emissions in the megacity. A list of CH<sub>4</sub> : CO<sub>2</sub> ratios reported by these observations is

shown in Table 4. These observations reported ratios ranging from 6.10 to 6.74 ppb CH<sub>4</sub> (ppm CO<sub>2</sub>)<sup>-1</sup> (Wennberg et al., 2012; Peischl et al., 2013; S. Newman, personal communication, 2014; Y.-K. Hsu, personal communication, 2014). At the California Institute of Technology (Caltech) in Pasadena and at the CLARS facility on Mount Wilson, in situ CH<sub>4</sub> and CO<sub>2</sub> mixing ratios were measured by two Picarro G1301 CO<sub>2</sub>–CH<sub>4</sub> analyzers (Newman et al., 2013). Secondary standards, calibrated against primary NOAA standards, were run every 11 h. Because of the complex boundary layer dynamics near mountains, measurements on Mount Wilson are influenced by upslope flow of air mass from the basin during the day and exposed to the clean background air from the free troposphere at night (Hsu et al., 2010). Using the mean of hourly averages from 22:00 to 03:00 PST on Mount Wilson



**Table 4.** Comparisons of CH<sub>4</sub> : CO<sub>2</sub> ratios and derived top-down CH<sub>4</sub> emissions among various measurements in the Los Angeles megacity. Wunch et al. (2009) reported two top-down CH<sub>4</sub> estimates:  $0.40 \pm 0.10 \text{ Tg CH}_4 \text{ year}^{-1}$  derived from the CH<sub>4</sub> : CO<sub>2</sub> ratio and  $0.60 \pm 0.10 \text{ Tg CH}_4 \text{ year}^{-1}$  derived from the CH<sub>4</sub> : CO ratio. Please note that it is difficult to compare the uncertainties due to the different measurement techniques.

Measurement (Location, period)	CH <sub>4</sub> : CO <sub>2</sub> ratio (ppb : ppm)	Derived top-down CH <sub>4</sub> emission (Tg CH <sub>4</sub> year <sup>-1</sup> )	Measurement type	References
TCCON (Pasadena, 8/2007–6/2008)	$7.80 \pm 0.80$	$0.40 \pm 0.10$ $0.60 \pm 0.10$	Column (FTS)	Wunch et al. (2009)
ARCTAS (LA, 6/2008)	$6.74 \pm 0.58$	$0.47 \pm 0.10$	Aircraft in situ (Picarro)	Wennberg et al. (2012)
CalNex (LA, 5/2010–6/2010)	$6.70 \pm 0.01$ $6.55 \pm 0.29$	$0.41 \pm 0.04$ $0.44 \pm 0.10$	Aircraft in situ (Picarro)	Peischl et al. (2013) Wennberg et al. (2012)
Caltech (Pasadena, 2/2012–8/2012)	$6.30 \pm 0.01$	$0.38 \pm 0.05$	Surface in situ	This study
Mount Wilson (Pasadena, 9/2011–6/2013)	$6.10 \pm 0.10$	$0.37 \pm 0.05$	Surface in situ (Picarro)	This study This study
CLARS-FTS, Mount Wilson (LA, 9/2011–10/2013)	$6.40 \pm 0.50$	$0.39 \pm 0.06$	Column (FTS)	This study

as the background reference, CH<sub>4</sub> and CO<sub>2</sub> excess mixing ratios were calculated by subtracting the background reference from the daytime hourly averaged measurements at Mount Wilson and at Caltech. The ratios were the correlation slopes between the two. Because of the different measurement techniques, measurement periods and locations, CH<sub>4</sub> : CO<sub>2</sub> ratios reported by these studies are not directly comparable to column measurements. However, the CLARS-FTS observations of CH<sub>4</sub> : CO<sub>2</sub> ratios show consistency with these measurements.

## 4 Discussion

### 4.1 Analysis assumptions

A number of assumptions are involved in deriving the CH<sub>4</sub> : CO<sub>2</sub> emission ratios. These are described in this subsection.

- XCH<sub>4(XS)</sub> and XCO<sub>2(XS)</sub> are correlated even though the two GHGs are not emitted from the same sources. CH<sub>4</sub> and CO<sub>2</sub> have chemical lifetimes that are much longer than the timescales for mesoscale transport and therefore behave like inert tracers in the boundary layer. Even if emitted from different sources, atmospheric processes in the boundary layer will result in mixing on relatively short timescales (a typical mixing timescale in the PBL is on the order of 10–20 min; Stull, 1988). CLARS-FTS samples air masses that have undergone this short-timescale mixing. The high degree of correlation observed between XCH<sub>4(XS)</sub> and XCO<sub>2(XS)</sub> for

all 28 reflection points supports this mixing assumption over the entire area of the LA basin.

- The slope of the XCH<sub>4(XS)</sub>–XCO<sub>2(XS)</sub> correlation observed at each LABS measurement point is sensitive to both the relative emissions over a horizontal path weighted toward the reflection point, and the composition of the air mass advected into the atmospheric path. The long optical path in the boundary layer and the effect of advection smear out the effects of local emission ratio variations. This smearing is different for each reflection point. Future work will deconvolve these effects using an atmospheric transport model, which will include advection, boundary layer mixing, surface emissions and ray tracing of the optical path sampled by CLARS-FTS on a 1–2 km grid.
- The effect of aerosol scattering on the XCH<sub>4(XS)</sub> : XCO<sub>2(XS)</sub> slopes is assumed to be negligible. Using a two-stream numerical radiative transfer model constrained by AERONET (AERosol NETwork) aerosol optical depths in the near infrared, Zhang et al. (2015) showed that the bias in the retrieved XCO<sub>2</sub> from CLARS-FTS LABS measurements does not exceed 1 %, using data that have passed the filter criteria described above. This bias is caused by the wavelength dependence of aerosol scattering and absorption between the CO<sub>2</sub> absorption band at 1.61 μm and the O<sub>2</sub> absorption band at 1.27 μm. Further analysis based on Zhang et al. (2015) indicates that the aerosol-induced bias on XCO<sub>2</sub> and XCH<sub>4</sub> is nearly identical and cancelled out in the ratio since the

CO<sub>2</sub> and CH<sub>4</sub> observations used in this analysis are retrieved at nearly identical wavelengths (1.61 μm vs. 1.66 μm). The uncertainty of the XCH<sub>4</sub> : XCO<sub>2</sub> ratio due to aerosol is negligible (<0.5 %). Uncertainties due to aerosol scattering on the CLARS-FTS XCO<sub>2</sub> and XCH<sub>4</sub> observations will be reduced significantly in the next version of the CLARS-FTS retrieval algorithm, which will consider aerosol scattering explicitly in the forward model (Zhang et al., 2015).

- The number of discrete reflection points (28 plus the direct solar path) is sufficient to characterize the average emission ratio over the Los Angeles megacity. The CLARS-FTS LABS mode spans slant distances in the range 4–40 km in the Los Angeles PBL and therefore should have sufficient spatial coverage of the megacity. In the future, sensitivity studies will be performed to optimize the spatial distribution of the reflection points with respect to coverage of emission sources, aerosol bias, albedo variability, locations of other stations in the monitoring network and other parameters.
- Seasonal bias in the XCH<sub>4(XS)</sub>–XCO<sub>2(XS)</sub> correlation slope is small. Certain times of the year are more likely to be influenced by cloud and aerosol events in Los Angeles and have correspondingly fewer measurements that pass the data quality filters. The fraction of data passing through the data filter varies by a factor of 2 in different seasons. In our analysis the effect of seasonal bias is small. This seems to be a reasonable assumption since a tight correlation was observed between XCH<sub>4(XS)</sub> and XCO<sub>2(XS)</sub> throughout the year; the contribution of seasonal sampling bias, if any, has a negligible effect on the random error of the annual average XCH<sub>4(XS)</sub>–XCO<sub>2(XS)</sub> correlation slope.
- Spatial variation in the atmospheric column of CO<sub>2</sub> and CH<sub>4</sub> above Mount Wilson is minimal and does not affect the XCH<sub>4</sub> : XCO<sub>2</sub> excess ratio. Spatial variation in the CO<sub>2</sub> and CH<sub>4</sub> mixing ratio above Mount Wilson in the basin is possible due to entrainment of boundary layer air mass into the free troposphere and long-range transport. It can be shown that spatial variability in the column above Mount Wilson due to entrainment of boundary layer height or long-range transport adds less than 1 % uncertainty to the XCH<sub>4</sub> : XCO<sub>2</sub> excess ratio.

#### 4.2 Top-down CH<sub>4</sub> emissions from CLARS-FTS observations

With the assumptions described in the previous subsection, we estimate the top-down annual CH<sub>4</sub> emission for the Los Angeles megacity based on the CLARS-FTS observations. In this analysis, we define the Los Angeles megacity as the spatial domain of the South Coast Air Basin.

The CARB reported an annual statewide CO<sub>2</sub> emission of 387 Tg CO<sub>2</sub> year<sup>−1</sup> for 2011 ([http://www.arb.ca.gov/app/ghg/2000\\_2011/ghg\\_sector.php](http://www.arb.ca.gov/app/ghg/2000_2011/ghg_sector.php)). Since the majority of CO<sub>2</sub> emissions are from fossil fuel combustion, we assumed that the CO<sub>2</sub> emissions are spatially distributed by population in the state. We apportioned the statewide emissions by population in the Los Angeles megacity, which is 43 % of statewide population, to estimate the bottom-up emission for the Los Angeles megacity (<http://www.census.gov/>). The bottom-up CO<sub>2</sub> emission inventory for the Los Angeles megacity was thus 166 ± 23 Tg CO<sub>2</sub> year<sup>−1</sup> in 2011, assuming 10 % uncertainties in both the CARB statewide CO<sub>2</sub> emission and the spatial distribution of emissions by population. For the bottom-up CH<sub>4</sub> emission in the Los Angeles megacity, we used the same method as in Wunch et al. (2009) and Peischl et al. (2013). The CARB reported an annual statewide CH<sub>4</sub> emission of 1.54 Tg CH<sub>4</sub> year<sup>−1</sup> for 2011 ([http://www.arb.ca.gov/app/ghg/2000\\_2011/ghg\\_sector.php](http://www.arb.ca.gov/app/ghg/2000_2011/ghg_sector.php)). Agriculture and forestry contributes 58 % of total CH<sub>4</sub> emission in the state (California Air Resources Board, 2011), but the Los Angeles basin contains less than 2 % of farmlands in California (United States Department of Agriculture, 2012). Therefore we estimated the bottom-up CH<sub>4</sub> emissions in the basin by subtracting the agriculture and forestry sector from the total statewide emission then apportioned by population. This gave a bottom-up CH<sub>4</sub> emission inventory of 0.28 Tg CH<sub>4</sub> year<sup>−1</sup> in the Los Angeles megacity in 2011. Using the bottom-up emission inventory of CO<sub>2</sub> for the Los Angeles megacity (166 ± 23 Tg CO<sub>2</sub> year<sup>−1</sup>) and the CH<sub>4</sub> : CO<sub>2</sub> ratio observed by the CLARS-FTS (6.4 ± 0.5 ppb CH<sub>4</sub> (ppm CO<sub>2</sub>)<sup>−1</sup>), we derived the CH<sub>4</sub> emission inventory using Eq. (3), where E<sub>CH<sub>4</sub>|top-down</sub> is the top-down CH<sub>4</sub> emissions inferred by the CLARS-FTS observations, E<sub>CO<sub>2</sub>|bottom-up</sub> is the bottom-up CO<sub>2</sub> emissions,  $\frac{XCH_4}{XCO_2}|_{slope}$  is the XCH<sub>4(XS)</sub> / XCO<sub>2(XS)</sub> ratio observed by the FTS and  $\frac{MW_{CO_2}}{MW_{CH_4}}$  is the ratio of molecular weight of CO<sub>2</sub> and CH<sub>4</sub> (that is, 16 g CH<sub>4</sub> / 44 g CO<sub>2</sub>).

$$E_{CH_4|top-down} = E_{CO_2|bottom-up} \times \frac{XCH_4}{XCO_2}|_{slope} \times \frac{MW_{CH_4}}{MW_{CO_2}} \quad (3)$$

The derived CH<sub>4</sub> emission inventory was 0.39 ± 0.06 Tg CH<sub>4</sub> year<sup>−1</sup> in the Los Angeles megacity assuming a 10 % uncertainty in the CARB bottom-up CO<sub>2</sub> emission. The derived CH<sub>4</sub> emission inventory was 18–61 % larger than the bottom-up emission inventory in 2011. This is in good agreement with the top-down CH<sub>4</sub> emissions from recent studies (Wunch et al., 2009; Hsu et al., 2010; Wennberg et al., 2012; Peischl et al., 2013; Jeong et al., 2013) and the CH<sub>4</sub> emissions derived from the observations at Caltech and on Mount Wilson (using the same bottom-up CO<sub>2</sub> emissions for the Los Angeles basin).

Because of the spatial and temporal variations of the CH<sub>4</sub> : CO<sub>2</sub> ratio in the Los Angeles megacity, the derived CH<sub>4</sub> emission based on local observations can be biased. For

instance, if we were to evaluate the bottom-up CH<sub>4</sub> emission inventory by our observations in west Pasadena only, the derived CH<sub>4</sub> emission inventory for the Los Angeles megacity would be overestimated by 14 %, since the west Pasadena target observed a CH<sub>4</sub> : CO<sub>2</sub> slope that is 14 % larger than the average slope of the 28 reflection points. Therefore, to quantify and to reduce uncertainties in carbon emissions from the Los Angeles megacity or any other urban areas which are highly heterogeneous, it is important to have measurements which provide both spatial and temporal coverage. It is challenging to quantify individual point sources of CH<sub>4</sub>. Further investigations need to be performed to link the CLARS-FTS observations to emissions from landfills, oil extraction and natural gas pipeline leakage.

### 4.3 Relevance to future satellite GHG observations

This study has shown that spatially resolved CH<sub>4</sub> : CO<sub>2</sub> emission ratio measurements can be made over a megacity domain (thousands of square kilometers) using a remote sensing method that simulates the observations from an imaging spectrometer such as GEO-FTS from geostationary orbit. From GEO, the field of regard is approximately one-third of the Earth below 60° latitude. Operating as a hosted payload from a commercial communications satellite, measurements of XCO<sub>2</sub>, XCH<sub>4</sub>, XCO and solar-induced chlorophyll fluorescence (SIF) will be made every 1–2 h during daylight with a pixel footprint of 2–3 km at the sub-satellite point with retrieval precisions comparable to those obtained from CLARS-FTS (Fu et al., 2014). In the near future, a two-dimensional imaging FTS similar to GEO-FTS will be deployed at CLARS to increase the spatial density of the retrievals.

## 5 Conclusions

This study is the first to map GHGs in the Los Angeles megacity using ground-based remote sensing technique. It combines the unique vista from Mount Wilson and high-sensitivity measurements made by the CLARS-FTS to simulate satellite observations. Persistent space- and time-resolved observations of GHG in the Los Angeles megacity over a 2-year period during 2011–2013 and a tracer-to-tracer correlation analysis are used to reveal an interesting spatial pattern of the CH<sub>4</sub> : CO<sub>2</sub> ratio in the megacity. The slope of the correlations between XCH<sub>4(XS)</sub> and XCO<sub>2(XS)</sub> showed significant spatial variations ranging from 5.4 to 7.3 ppb CH<sub>4</sub> (ppm CO<sub>2</sub>)<sup>-1</sup>, with an average of 6.4 ± 0.5 ppb CH<sub>4</sub> (ppm CO<sub>2</sub>)<sup>-1</sup>, indicating that there is spatial heterogeneity in the megacity. Using the CARB bottom-up emission inventory of CO<sub>2</sub>, we derived the CH<sub>4</sub> emission inventory of the Los Angeles megacity during 2011–2013 to be 0.39 ± 0.06 Tg CH<sub>4</sub> year<sup>-1</sup>, which was 18–61 % above the bottom-up CH<sub>4</sub> emission inventory. Good agreement among

previous aircraft observations and local observations indicated that CLARS-FTS provides accurate measurements that can efficiently quantify and track GHG emissions in the Los Angeles megacity. Due to the complexity of the measurement geometry of the CLARS-FTS observations, it is challenging to pinpoint local sources with high precision. However, the CLARS-FTS observations, which span the Los Angeles megacity continuously, fill the gap between the surface in situ measurements that can provide long-term localized observations, and aircraft measurements which provide vertical profile information but are made infrequently. The ideal monitoring system will combine remote sensing observations, such as those from CLARS, with in situ ground and aircraft data to achieve a calibrated, long-term data set for the estimation of GHG emissions trends.

*Acknowledgements.* The authors thank our colleagues at JPL, Q. Zhang (California Institute of Technology), D. Wunch (California Institute of Technology), P. Wennberg (California Institute of Technology), C. Roehl (California Institute of Technology), J. Stutz (University of California, Los Angeles) and G. Keppel-Aleks (University of Michigan) for helpful comments. Support from the NASA Postdoctoral Program, California Air Resources Board, NOAA Climate Program, NIST GHG and Climate Science Program and JPL Earth Science and Technology Directorate is gratefully acknowledged. Y. L. Yung was supported in part by NASA grant NNX13AK34G to the California Institute of Technology and the KISS program of Caltech.

Edited by: R. Harley

## References

- Aben, I., Hasekamp, O., and Hartmann, W.: Uncertainties in the space-based measurements of CO<sub>2</sub> columns due to scattering in the Earth's atmosphere, *J. Quant. Spectrosc. Ra.*, 104, 450–459, 2007.
- California Air Resources Board: Greenhouse gas emission inventory – Query tool for years 2000 to 2011, 6th Edn., [http://www.arb.ca.gov/app/ghg/2000\\_2011/ghg\\_sector.php](http://www.arb.ca.gov/app/ghg/2000_2011/ghg_sector.php), (last access: January 2014), 2011.
- Crisp, D., Fisher, B. M., O'Dell, C., Frankenberg, C., Basilio, R., Bösch, H., Brown, L. R., Castano, R., Connor, B., Deutscher, N. M., Eldering, A., Griffith, D., Gunson, M., Kuze, A., Mandrake, L., McDuffie, J., Messerschmidt, J., Miller, C. E., Morino, I., Natraj, V., Notholt, J., O'Brien, D. M., Oyafuso, F., Polonsky, I., Robinson, J., Salawitch, R., Sherlock, V., Smyth, M., Suto, H., Taylor, T. E., Thompson, D. R., Wennberg, P. O., Wunch, D., and Yung, Y. L.: The ACOS CO<sub>2</sub> retrieval algorithm – Part II: Global X<sub>CO<sub>2</sub></sub> data characterization, *Atmos. Meas. Tech.*, 5, 687–707, doi:10.5194/amt-5-687-2012, 2012.
- de la Rue du Can, S., Wenzel, T., and Price, L.: Improving the Carbon Dioxide Emission Estimates from the Combustion of Fossil Fuels in California, Report prepared for the California Air Resources Board and the California Environmental Protection Agency, 1–52, 2008.

- Efron, B. and Tibshirani, R.: An Introduction to the Bootstrap, Vol. 57, CRC press, Boca Raton, Florida, USA, 45–82, 1993.
- Fu, D., Pongetti, T. J., Blavier, J.-F. L., Crawford, T. J., Manatt, K. S., Toon, G. C., Wong, K. W., and Sander, S. P.: Near-infrared remote sensing of Los Angeles trace gas distributions from a mountaintop site, *Atmos. Meas. Tech.*, 7, 713–729, doi:10.5194/amt-7-713-2014, 2014.
- Hsu, Y.-K., VanCuren, T., Park, S., Jakober, C., Herner, J., FitzGibbon, M., Blake, D. R., and Parrish, D. D.: Methane emissions inventory verification in southern California, *Atmos. Environ.*, 44, 1–7, 2010.
- Jeong, S., Hsu, Y.-K., Andrews, A. E., Bianco, L., Vaca, P., Wilczak, J. M., and Fischer, M. L.: A multitower measurement network estimate of California's methane emissions, *J. Geophys. Res.-Atmos.*, 118, 11339–11351, doi:10.1002/jgrd.50854, 2013.
- Key, R., Sander, S., Eldering, A., Blavier, J.-F., Bekker, D., Manatt, K., Rider, D., and Wu, Y.-H.: The geostationary fourier transform spectrometer, *Proc. SPIE*, 8515, doi:10.1117/12.930257, 2012.
- Kort, E. A., Angevine, W. M., Duren, R., and Miller, C. E.: Surface observations for monitoring urban fossil fuel CO<sub>2</sub> emissions: Minimum site location requirements for the Los Angeles megacity, *J. Geophys. Res.-Atmos.*, 118, 1577–1584, doi:10.1002/jgrd.50135, 2013.
- Mandrake, L., Frankenberg, C., O'Dell, C. W., Osterman, G., Wennberg, P., and Wunch, D.: Semi-autonomous sounding selection for OCO-2, *Atmos. Meas. Tech.*, 6, 2851–2864, doi:10.5194/amt-6-2851-2013, 2013.
- Newman, S., Jeong, S., Fischer, M. L., Xu, X., Haman, C. L., Lefler, B., Alvarez, S., Rappenglueck, B., Kort, E. A., Andrews, A. E., Peischl, J., Gurney, K. R., Miller, C. E., and Yung, Y. L.: Diurnal tracking of anthropogenic CO<sub>2</sub> emissions in the Los Angeles basin megacity during spring 2010, *Atmos. Chem. Phys.*, 13, 4359–4372, doi:10.5194/acp-13-4359-2013, 2013.
- O'Dell, C. W., Connor, B., Bösch, H., O'Brien, D., Frankenberg, C., Castano, R., Christi, M., Eldering, D., Fisher, B., Gunson, M., McDuffie, J., Miller, C. E., Natraj, V., Oyafuso, F., Polonsky, I., Smyth, M., Taylor, T., Toon, G. C., Wennberg, P. O., and Wunch, D.: The ACOS CO<sub>2</sub> retrieval algorithm – Part 1: Description and validation against synthetic observations, *Atmos. Meas. Tech.*, 5, 99–121, doi:10.5194/amt-5-99-2012, 2012.
- Peischl, J., Ryerson, T. B., Brioude, J., Aikin, K. C., Andrews, A. E., Atlas, E., Blake, D., Daube, B. C., de Gouw, J. A., Dlugokencky, E., Frost, G. J., Gentner, D. R., Gilman, J. B., Goldstein, A. H., Harley, R. A., Holloway, J. S., Kofler, J., Kuster, W. C., Lang, P. M., Novelli, P. C., Santoni, G. W., Trainer, M., Wofsy, S. C., and Parrish, D. D.: Quantifying sources of methane using light alkanes in the Los Angeles basin, California, *J. Geophys. Res.-Atmos.*, 118, 4974–4990, doi:10.1002/jgrd.50413, 2013.
- Sibson, R.: A brief description of natural neighbor interpolation, in: *Interpreting Multivariate Data*, edited by: Barnett, V., Wiley, Chichester, 21–36, 1981.
- Spurr, R. J.: VLIDORT: A linearized pseudo-spherical vector discrete ordinate radiative transfer code for forward model and retrieval studies in multilayer multiple scattering media, *J. Quant. Spectrosc. Ra.*, 102, 316–342, 2006.
- Stull, R.: *An Introduction to Boundary Layer Meteorology*, Springer, the Netherlands, 2–67, 1988.
- United States Department of Agriculture: The Census of Agriculture: Census Publications, technical report, US Dep. Agric., Washington, DC, available at: [http://www.agcensus.usda.gov/Publications/2012/Full\\_Report/Volume\\_1,\\_Chapter\\_2\\_County\\_Level/California/st06\\_2\\_001\\_001.pdf](http://www.agcensus.usda.gov/Publications/2012/Full_Report/Volume_1,_Chapter_2_County_Level/California/st06_2_001_001.pdf) (last access: August 2014), 2012.
- Washenfelder, R. A. and Wennberg, P. O.: Tropospheric methane retrieved from ground-based near-IR solar absorption spectra, *Geophys. Res. Lett.*, 30, 2226, doi:10.1029/2003GL017969, 2003.
- Washenfelder, R. A., Toon, G. C., Blavier, J.-F., Yang, Z., Allen, N. T., Wennberg, P. O., Vay, S. A., Matross, D. M., and Daube, B. C.: Carbon dioxide column abundances at the Wisconsin Tall Tower site, *J. Geophys. Res.*, 111, D22305, doi:10.1029/2006JD007154, 2006.
- Wennberg, P. O., Mui, W., Wunch, D., Kort, E. A., Blake, D. R., Atlas, E. L., Santoni, G. W., Wofsy, S. C., Diskin, G. S., Joeng, S., and Fischer, M. L.: On the sources of methane to the Los Angeles atmosphere, *Environ. Sci. Technol.*, 46, 9282–9289, doi:10.1021/es301138y, 2012.
- Wunch, D., Wennberg, P. O., Toon, G. C., Keppel-Aleks, G., and Yavin, Y. G.: Emissions of greenhouse gases from a North American megacity, *Geophys. Res. Lett.*, 36, L15810, doi:10.1029/2009GL039825, 2009.
- Wunch, D., Toon, G. C., Blavier, J. L., Washenfelder, R. A., Notholt, J., Connor, B. J., Griffith, D. W., Sherlock, V., and Wennberg, P. O.: The total carbon column observing network, *Philos. T. Roy. Soc. A*, 369, 2087–2112, 2011.
- Yoshida, Y., Ota, Y., Eguchi, N., Kikuchi, N., Nobuta, K., Tran, H., Morino, I., and Yokota, T.: Retrieval algorithm for CO<sub>2</sub> and CH<sub>4</sub> column abundances from short-wavelength infrared spectral observations by the Greenhouse gases observing satellite, *Atmos. Meas. Tech.*, 4, 717–734, doi:10.5194/amt-4-717-2011, 2011.
- Zhang, Q., Natraj, V., Li, K., Shia, R., Fu, D., Pongetti, T., Sander, S. P., and Yung, Y. L.: Influence of aerosol scattering on the retrieval of CO<sub>2</sub> mixing ratios: a case study using measurements from the California Laboratory for Atmospheric Remote Sensing (CLARS), *Geophys. Res. Lett.*, in preparation, 2015.